ACS OMEGA

Open Access

http://pubs.acs.org/journal/acsodf

Article

Chemometric Analysis Combined with GC × GC-FID and ESI HR-MS to Evaluate Ultralow-Sulfur Diesel Stability

Deborah V. A. de Aguiar, Jussara V. Roque,* Leomir A. S. de Lima, Iris M. Junior, Helineia O. Gomes, Emanoel N. R. de Sousa, Gláucia P. L. Piccoli, and Boniek G. Vaz*

Cite This: *ACS Omega* 2024, 9, 10415−10425

Read Online

ACCESS | Metrics & More | Article Recommendations | Supporting Information

ABSTRACT: Diesel has been the most employed fuel in highway and nonhighway transportation systems. Many studies over the past years have attempted to classify diesel as a stable or unstable composition since this fuel can still degrade during storage or thermal oxidative processes. Products generated because of such degradation are the reason for the formation of soluble gums and insoluble organic particulates, which in turn cause a negative influence on engine performance. This work reports a detailed composition of nonpolar and polar compounds in many ultralow-sulfur diesel (ULSD) samples by comprehensive two-dimensional gas chromatography with a flame ionization detector (GC × GC-FID) and electrospray ionization high-resolution mass spectrometry (ESI HR-MS). In addition, chemometric approaches were applied for ULSD storage stability investigation. GC × GC-FID experiments achieved the nonpolar chemical characterization for the ULSD samples, including all main hydrocarbon classes: paraffins, mono- and dinaphthenics and olefins, and aromatics. The GC × GC-FID data combined with principal component analysis (PCA) described that the separation of the samples' concerning storage stability was mainly due to the contents of mono- and diaromatic compounds in the unstable ULSD samples. Moreover, PCA was also applied to the ESI (±) data set, and the results highlight the presence of compounds belonging to O class (natural antioxidants), which decrease the rate of oxygen consumption in the fuel, characterizing it as stable composition. The basic nitrogen compounds are mostly present in the stable ULSD samples indicating that they did not affect the stability of the fuel. On the other hand, the HC classes presented pronounced abundance among unstable ULSD samples suggesting that the fuel degradation may go through the oxidation of hydrocarbons and the formation of O_x compounds as byproducts. Furthermore, MS/MS experiments point to the formation of $C_cH_hN_nO_o$-like precursor species, which can react with each other and lead to the formation of gums and insoluble sediments in the fuel. In summary, the results express the potential of using the GC × GC-FID and ESI (±) Orbitrap MS techniques as valuable tools for diesel stability evaluations.

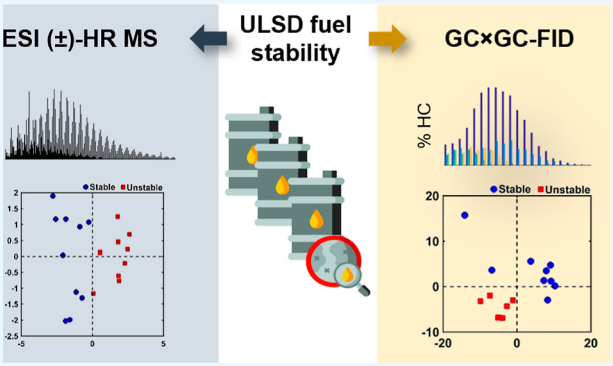

1. INTRODUCTION

In the last few years, diesel was considered the most refined product produced in Europe, and in 2022, its consumption by the United States transportation sector was approximately 3 million barrels per day.[1,2] This middle distillate fuel is composed of a complex mixture containing aromatic, paraffinic, olefinic, and naphthenic hydrocarbons, besides compounds containing nitrogen, sulfur, and oxygen atoms (NSO).[3]

Many studies have identified diesel as a stable or unstable composition,[4−6] and the proportion between the displayed classes of compounds directly influences diesel performance. Consequently, diesel can degrade during storage or thermal oxidation processes involving soluble gums and insoluble organic particulates.[7−10] The degradation process in middle distillates ranges from several oxidative and polymerization reactions, inorganic compounds, additives, and fillers added during refining to the fuel chemical predisposition to instability through free-radical mechanism.[10]

Fundamental studies on the oxidative degradation of middle distillate fuels have been reported by many authors.[8,11−13] In 2005, Beaver et al.[14] proposed a mechanistic study where aromatic heteroatomic species such as phenols and arylamines can undergo oxidation. Consequently, quinone species are formed, which can function as electrophiles in nonoxidized compounds in the coupling reactions generating soluble macromolecular oxidatively reactive species (SMORS). There-

Received: October 23, 2023
Revised: December 22, 2023
Accepted: February 9, 2024
Published: February 21, 2024

fore, solubility decrease was the driving force for these compounds' precipitation and their contribution to deposit formation. SMORS mechanism for middle distillates is described in Scheme S1 (see the Supporting Information).

In a similar manner, Balster et al.[15] presented that the trend of oxidative thermal deposition is proportional to the polar species level current in the fuel. However, the formation of deposits in a specific fuel depends on the classes of polar compounds. The authors observed that fuels with a high content of anilines, quinolines, and pyridines result in less deposit formation than fuels with the same total polar content, mainly phenols, carbazoles, and indoles. Correspondingly, Siddiquee and Klerk[16] studied oxidative reactions of compounds containing nitrogen, oxygen, and sulfur atoms at 130 °C. The authors found that heterocyclic compounds containing five-membered rings are more vulnerable to oxidative reactions than acyclic structures and six-membered rings. Among the five-membered heterocyclic compounds, the tendency to form oxidative products was N > O ≫ S.

Therefore, diesel stability has been a significant concern due to its direct impact on the performance of diesel engines. It currently undergoes extensive standard laboratory test methods (e.g., ASTM D2274[17] e D5304[18]) to verify its stability before use. Stability denotes the fuel's resistance to changes in its original chemical composition when it is stored for long periods (storage stability) or exposed to high temperatures in a short period (thermal stability), and there is no appreciable deterioration in its chemical composition.[19,20]

Recently, there has been a notable increase in the production of ultralow-sulfur diesel (ULSD). This surge is primarily driven by stringent environmental regulations and modifications in nonhighway diesel fuel legislation implemented by the International Maritime Organization.[21,22] To meet these standards, the sulfur content of the diesel fuel was reduced for values in the range of 10−15 ppm. ULSD production is commonly achieved by hydrotreatment (HDT), and it directly affects the chemical composition of the final product.[23] Therefore, it is necessary to understand the different chemical compositions that differentiate the ULSD's stability from instability.

Several analytical techniques have been used in the chemical characterization of petroleum and its derivatives.[24−26] Detailed determination of nonpolar composition in middle distillates has been achieved by comprehensive two-dimensional gas chromatography (GC × GC).[27] In this technique, the fuel could be separated into components employing two capillary columns with different stationary phases.[28,29]

Maximilian et al. reported the application of GC × GC−time-of-flight mass spectrometry (GC × GC−TOF MS) for the group-type quantification of middle distillates.[30] The same authors also evaluated in another approach the normal and reversed phase column combinations for GC × GC−TOF MS for the analysis of commercially available middle distillates. The authors concluded that the reversed phase provides advantages for the quantification of petrochemical samples in terms of precision of the results.[31] In addition, GC × GC with a flame ionization detector (FID) has been widely applied for hydrocarbon quantitative purposes.[27,32]

However, there is a limitation concerning their resolving power when a compositional detail at the molecular level is desired. In this context, the advent of high-resolution mass spectrometry (HR-MS) allowed new horizons for the petrochemical industry. HR-MS has enabled a more comprehensive characterization of less abundant species in oil, especially when electrospray ionization (ESI) is the ionization source.[33−37] ESI HR-MS successfully performs the analysis of polar compounds present in petroleum and its derivatives based on its ability to ionize and characterize basic and acidic compounds selectively.[38−40] Therefore, the ESI HR-MS technique has been employed as a valuable tool for characterizing the polar chemical composition and assessing the stability of middle distillates.[20,41,42]

Generally, compositional characteristics that can affect fuel properties are often hidden by an abundance of nonrelevant information. Therefore, the chemometric techniques seem to be suitable for revealing hidden information from fuel composition data obtained by different analytical techniques. Several studies have focused on discriminating different fuel proprieties using chemometric procedures.[43−46] Multivariate exploratory analysis has been employed to examine petroleum-derived properties such as principal component analysis (PCA).[45−47] The PCA is a method that reduces data dimensionality and reveals more prominent and significant patterns of variation for a given data set.[48] Hence, PCA can be used to identify clusters of similar samples. However, their potential is not widely explored for monitoring ULSD stability.[49]

In this regard, this paper reports the use of GC × GC-FID and ESI (±) HR-MS for the characterization of the nonpolar and polar composition of ULSD samples. Chemometric approaches were applied to both techniques to identify potential compound classes which cause ULSD samples' instability during storage.

2. MATERIALS AND METHODS

2.1. ULSD Samples. ULSD samples were classified as stable (S-ULSD, 10 samples) and unstable (U-ULSD, 10 samples) by the *Standard Test Method for Assessing Middle Distillate Fuel Storage Stability by Oxygen Overpressure* (ASTM D5304) and were supplied by the Centre of Research, Development, and Innovation Leopoldo Américo Miguez de Mello (CENPES, Petrobras, RJ, Brazil). The ASTM D5304 has been employed as a standard method to assess the storage stability of middle distillates in the presence of oxygen. The test was conducted in glass under standardized conditions: a temperature of 90 °C and a pressure of 800 kPa O_2 over a period of 16 h. The precipitate generated was filtered and weighed. It was required that for stable samples, the amount of insoluble sediments measured was not more than 0.1 mg for every 100 mL of the fuel.[50]

2.2. Elemental Analysis. The total nitrogen content was determined by the boat-inlet chemiluminescence method in accordance with ASTM D5762-18,[51] whereas carbon and hydrogen were determined concurrently in a single instrumental procedure according to ASTM D5291-1.[52]

2.3. Two-Dimensional Gas Chromatography: Instrument Parameters. GC × GC was performed using an Agilent 7890A gas chromatographic oven equipped with a capillary flow modulator. The first-dimension column was an Agilent J&W fused silica capillary column, 15 m × 0.25 mm, with a DB-5MS stationary phase of 0.25 μm film thickness. The second-dimension column was an Agilent fused silica capillary column, 5 m × 0.25 mm, with a DB-17MS stationary phase of 0.25 μm film thickness. Hydrogen gas was used as the carrier gas with a flow rate of about 0.2 mL min^{-1}. A total of 0.5 μL of each sample—S-ULSD (9 samples) and U-ULSD (7

https://doi.org/10.1021/acsomega.3c08336
ACS Omega 2024, 9, 10415−10425

samples)—was injected pure, and the samples' introduction was made using a split/splitless injector with a 100:1 split ratio at 320 °C. The GC oven was ramped at 2 °C min^{-1} from 40 °C (1 min) to 310 °C (10 min). The modulation period was set to 6 s. The FID parameters were detected at a temperature of 320 °C, a hydrogen flow rate of 30 mL min^{-1}, an air flow of 300 mL min^{-1}, and a makeup gas flow (nitrogen) of 20 mL min^{-1}. The GC × GC-FID experiments for one stable ULSD sample (S-ULSD 7) and three unstable ULSD samples (U-ULSD 3, 9, and 10) were not performed since they ran out during the study.

2.4. ESI HR-MS: ULSD Sample Preparation and Instrument Parameters. A total of 20 μL of each ULSD sample was diluted to 1 mL of toluene/methanol (70:30, v/v) solution. Ammonium hydroxide (NH_4OH) was added (5 μL to every 1 mL of sample solution) to ensure efficient ionization for negative-ion mode ESI analysis. In the same proportion, formic acid (HCOOH) was added in the positive-ion mode. HPLC grade toluene and methanol used were provided by J. T. Baker (Phillipsburg, NJ, United States).

The ESI MS analysis was performed employing a Q-Exactive Orbitrap (Thermo Scientific, Bremen, Germany) with a commercial heated ESI source (HESI). Samples were loaded into a 500 μL syringe (Hamilton) and directly infused using an integrated syringe pump at a flow of 3.0 μL min^{-1}. The ion source was operated using the following parameters: spray voltage of 3.2 and 3.5 kV for the negative- and positive-ion mode, respectively; mass range from m/z 100 to 600 for the negative mode and m/z 100 to 800 for the positive mode; sheath gas: 5; S-lens: 50; capillary temperature: 275 °C; aanutomatic gain control (AGC) target: 1×10^6 (full scan) and 5×10^5 (MS/MS); maximum injection time (IT): 50 ms (full scan) and 200 ms (MS/MS); and microscans: 5. For the MS/MS experiments, N_2 was employed as the collision gas and the improved energy collision dissociation (HCD) was wide-ranging from 25 to 45 normalized collision energy (NCE) to enhance the ion current in the spectra with an isolation window of m/z 0.2. The resolving power was set to 140,000 (fwhm at m/z 200). The Xcalibur version 2.2 (Thermo Fisher Scientific, CA, United States) software was employed for instrument control/data acquisition.

The Composer software (Sierra Analytics, CA, United States) version 1.5.3 was employed to assign molecular formulas of the detected ions. This step was carried out to group the compounds identified by the heteroatom type, series (hydrogen deficiency−double bond equivalent (DBE)), and degree of alkylation (carbon number) and also to evaluate the chemical information in the data set previous to chemometric modeling. Composer formula assignments were fixed between m/z 100 and 1400, based on the number of atoms: 200 C, 400 H, 4 N, 4 O, and 4 S according to the walking recalibration equation. The assignment process followed hydrocarbon rules to generate meaningful chemical formulas and a mass error tolerance of 5 ppm. All assignable molecular formulas for each crude oil were exported to Microsoft Excel 2016 and then imported to Origin 2018 for analysis.

2.5. Data Analysis. Chemometric approaches were applied in GC × GC-FID and ESI HR-MS data sets separately to gain comprehensive understanding of the sample composition. For the first one, an **X** matrix containing 16 samples and six variables (hydrocarbon compound classes) was built to perform PCA. This approach enabled us to perform PCA at the class level, rather than on individual species, facilitating a more interpretable analysis of the complex hydrocarbon profiles. In this matrix, values of 0 (zero) were assigned to specific hydrocarbon compound classes in cases where they were detected in some samples but absent in others, ensuring a comprehensive data set for analysis. In contrast, the ESI (±) HR-MS data set was more extensive, comprising 20 samples with a total of 1560 variables (compounds that were detected in both ionization modes). These variables represented individual compounds detected across both ionization modes, allowing us to perform PCA on a detailed level to capture the full chemical diversity within the samples. For this data set, a similar approach was adopted where missing values were set to 0 (zero) for compounds detected in some samples under both ionization modes but not in others. The $\mathbf{X}_{20\times1560}$ matrix was created; of the total 1560 variables, 449 of them were obtained by ESI (−) analysis and 1111 by ESI (+). Both modes were imported separately. To integrate these two ESI data sets, a low-level data fusion approach was employed. This process began with the separate preprocessing of each ESI data set to preserve their distinct characteristics. Following preprocessing, the data sets were concatenated, forming a combined data set for PCA. This method was chosen to ensure that the comprehensive nature of each data set was maintained, enabling a holistic analysis.

The pretreatment and application of PCA were implemented in the MATLAB R2020a software (MathWorks Inc., MA, USA). Normalization and mean centering were applied to both data sets before performing PCA. For the GC × GC-FID data set, autoscale preprocessing was exclusively used to ensure appropriate scaling of the variables. In contrast, the ESI HR-MS data sets (both positive and negative ionization modes) underwent a distinct preprocessing approach, where normalization and mean centering were applied prior to data fusion. This tailored preprocessing for each data set was crucial to accurately reflect the unique characteristics of the data in each analytical method, thereby ensuring the robustness and reliability of the subsequent PCA.

The reduction of the number of variables by the PCA application was achieved by decomposing the original matrix **X** into its matrix products in scores and loadings, as shown in eq 1

$$\mathbf{X} = \mathrm{TP}^{\mathrm{T}} + \mathbf{E} \tag{1}$$

where **X** is the matrix $I \times J$ (I is the number of samples and J is the number of variables); **T** is the matrix of vector scores t_a $I \times A$ (A is the number of computed components); **P** is the matrix of vector loadings $J \times A$ (the superscript T indicates the transposed matrix P); and **E** is the residual matrix $I \times J$.

3. RESULTS AND DISCUSSION

The elemental composition of the 20 ULSD samples is described in Table S1 (see the Supporting Information). In general, the contents of carbon and hydrogen among the ULSD samples were similar. However, the same cannot be applied to the total nitrogen content. Considering the average between the set of ULSD samples, it was observed that the total nitrogen content for unstable ULSD samples was higher than for the stable ULSD samples, with values of 16.0 and 1.9 mg kg^{-1}, respectively.

As it is known, the level of polar species could be correlated with the thermal oxidative deposition tendency in middle distillates,[16] even though the classes of the polar species also affected the amount of deposits produced by a specific fuel.

https://doi.org/10.1021/acsomega.3c08336
ACS Omega 2024, 9, 10415−10425

Generally, fuels with high levels of basic nitrogen content were likely to generate fewer deposits than those with the same polar content but consisting of nonbasic nitrogen compounds.[15,16] However, the total nitrogen content determined by the boat-inlet chemiluminescence method cannot differentiate between the basic and nonbasic nitrogen compounds. Therefore, the influence of these compound classes will be discussed later, in which the results of mass spectrometry analyses will be shown.

3.1. GC × GC-FID. GC × GC has been applied to the analysis of different petroleum-derived samples.[53−55] The use of two chromatographic dimensions allows compound separation based on their polarity and volatility. When combined with FID, GC × GC becomes a powerful technique for the speciation and determination of hydrocarbons in different types of samples.[27] In this way, they are arranged according to their chemical group and their amount of carbon atoms.[54]

GC × GC-FID experiments achieved the main hydrocarbon classes: paraffins, mono- and dinaphthenics, olefins, and aromatics, as described in Table S2 (see the Supporting Information). Our GC × GC-FID method cannot differentiate between olefins and mono- and dinaphthenics. Therefore, they were grouped and referred to as "mononaphthenics and olefins" and "dinaphthenics and olefins". However, as ULSD is a hydrotreated fuel, the olefin content is expected to be minimal.[27] Hence, the contents of the classes of hydrocarbons referred to as "mononaphthenic and olefins" and "dinaphthenics and olefins" may be mostly related to the mononaphthenic and dinaphthenic contents.

The results from GC × GC-FID were evaluated to investigate which hydrocarbon classes are most significant for ULSD stability classification. PCA was applied to a matrix of 16 samples containing the total content of each main hydrocarbon class. PCA scores from principal components 1 and 2 are shown in Figure 1A. The dashed ellipse delineates

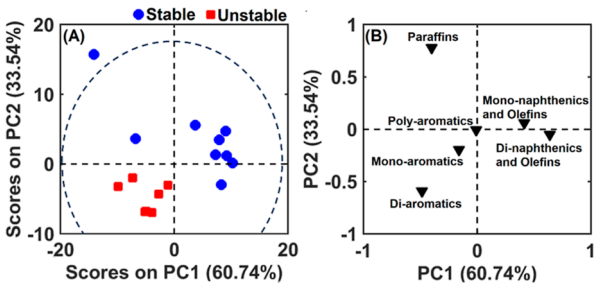

Figure 1. (A) Scores and (B) loadings for the GC × GC-FID for 16 ULSD samples analyzed by PCA. The dashed ellipse delineates the 95% confidence region.

the 95% confidence region in the PCA score plot, with one sample notably positioned outside this boundary, indicating a deviation from the general sample clustering. A total of 94.28% of the data variance was explained considering the two main components, and the separation of stable and unstable ULSD samples was observed in both components.

PCA allowed to identify patterns in the data set and express the data in such a way as to highlight their similarities and differences. According to Figure 1B, the major difference between stable and unstable ULSD samples is the content of mono- and diaromatics. These findings corroborate the total contents of the main hydrocarbon classes described in Table S2 (see the Supporting Information). The unstable ULSD samples exhibited the content of mono- and diaromatics in the range of 21.21−25.58 and 3.92−7.32 in %, w/w by comparison of the values of 10.87−18.27 and 0.59−3.43 in %, and w/w for stable ULSD samples, respectively. By contrast, loadings referring to mono- and dinaphthenics mainly categorize the stable samples.

The high contents of mono- and diaromatic hydrocarbons observed for the unstable ULSD samples may be an indicator of the reason that these samples exhibited unstable performance when subjected to the induced storage test in accordance with ASTM D5304. Dewitt et al. observed that the content of aromatic hydrocarbons as well as the amount of fused aromatic rings are intrinsically related to the amount of deposits formed in a commercial fuel.[56]

Table S2 (see the Supporting Information) describes that the contents attributed to hydrocarbons containing more than two fused aromatic rings, or even lower, were determined in higher proportions for the unstable ULSD samples. This can also be associated with the unstable performance observed for these samples. In general, the low values found for this class of compounds in the ULSD samples may be related to the hydrogenation process characteristic of HDT, where aromatic hydrocarbons are converted into their saturated analogues and paraffins.[55]

On the other hand, the loadings for mono- and dinaphthenics mainly categorize the stable ULSD samples. The majority of the presence of these two classes of hydrocarbons among the stable samples also suggests that the olefin content is minimal among the ULSD samples. Olefins are the class of hydrocarbons most susceptible to the formation of gums and deposits in the fuel, given that this class of compounds is more reactive to oxidation reactions.[42] Consequently, the presence of olefins in the set of stable samples would lead to the formation of precipitates during the induced storage experiment, exceeding the recommended value according to ASTM D5304, which was not observed for these samples.

Figures S1 and S2 (Supporting Information) show the distribution plots of the carbon number vs the content of the main hydrocarbon classes for the stable and unstable ULSD samples accessed by GC × GC-FID, respectively. The detected carbon number range included values between C_5 and C_{30} for all ULSD samples. Among the stable samples, S-ULSD 1 had an outstanding profile from the others (this sample has a score higher than 10 in PC2—Figure 1), and precisely, the paraffin content contributes to this separation, as can be seen in loadings from Figure 1B. It has been reported that the presence of paraffins in fuel does not affect its stability, since this type of hydrocarbon has a low susceptibility to oxidation.[57]

In addition, Figure S1 (see the Supporting Information) also points out similar carbon number distributions among the samples S-ULSD 2, 3, 6, and 8. In contrast, for S-ULSD 4, 5, 9, and 10, monoaromatic distribution stood out with more prominent content in compounds with carbon numbers of C_{14} and C_{15}. Conversely, the carbon number distribution profile among the unstable samples (Figure S2, see the Supporting Information) was similar except for U-ULSD 1 and 6, which showed an increase in the paraffin, mono- and dinaphthenic, and olefin contents in the region between C_8 and C_{12}.[58]

Although, it is also necessary to evaluate the polar composition of these samples, which cannot be accessed using the GC × GCt-FID technique. Hence, the ESI (±)

https://doi.org/10.1021/acsomega.3c08336
ACS Omega 2024, 9, 10415−10425

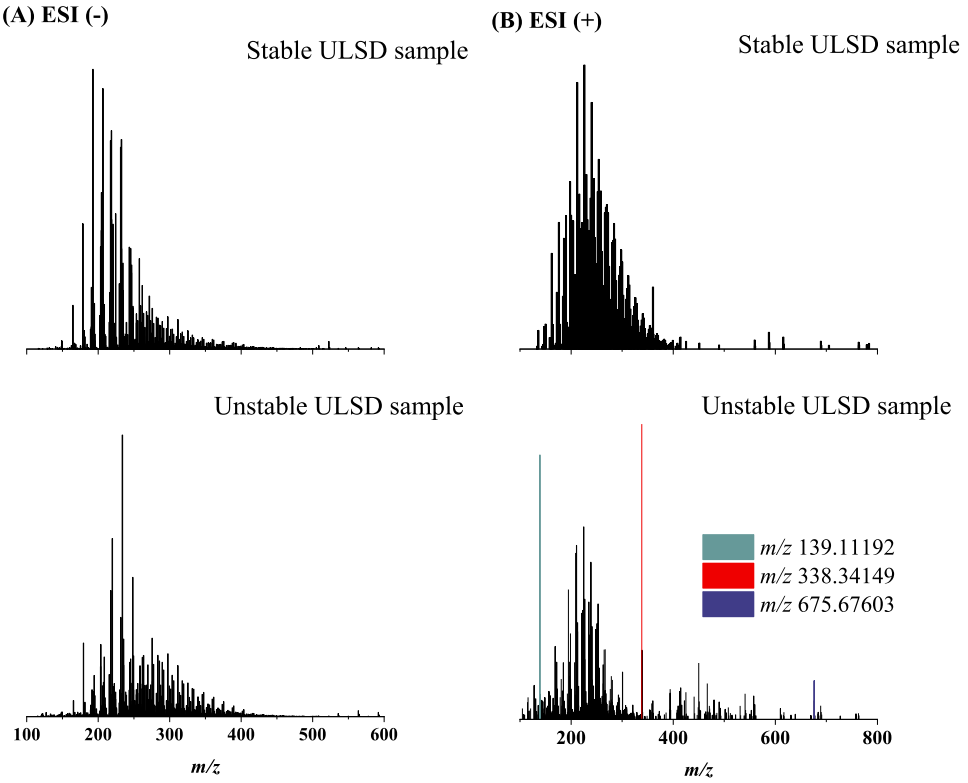

Figure 2. (A) Negative-ion mode ESI mass spectra for stable and unstable ULSD samples. (B) Positive-ion mode ESI mass spectrum profile in the m/z 100−600 range for stable and unstable ULSD samples.

Orbitrap MS was employed in order to understand the distribution of polar compounds in ULSD samples.

3.2. ESI (±) HR-MS. ESI (±) Orbitrap MS was applied to the chemical characterization of the ULSD samples and further correlated with their storage stability in accordance with ASTM D5304. The number of assigned peaks and assigned percentage (%) for all ULSD samples in both ion mode ionization is described in Table S3 (see the Supporting Information). The error distribution as a function of m/z for stable and unstable ULSD samples is illustrated in Figures S3 and S4 (see the Supporting Information) for the negative-ion mode and Figures S5 and S6 for the positive-ion mode, respectively (see the Supporting Information).

The ESI (−) mass spectra, Figure 2A, illustrated the stable and unstable mass spectra presented over the entire m/z range, from 100 to 600. Highlighted in Figure 2A, the mass spectrum for the unstable ULSD sample exhibited most of the peaks concentrated in the spectral region ranging between m/z 200 and 400.

The ESI (+) mass spectra for stable and unstable diesel illustrated in Figure 2B showed the m/z range from 100 to 800. For the stable diesel, most peaks were centered in the spectral area ranging between m/z 100 and 400. However, as seen in the mass spectrum for the unstable diesel, the mass range detected included m/z 100 and 300. In addition, the presence of intense ions is notable, which were m/z 139.11192, 338.34149, and 675.67603, corresponding to $C_9H_{15}O^+$, $C_{22}H_{44}ON^+$, and $C_{44}H_{87}O_2N_2^+$. We supposed that these last ions that do not pertain to any measured homologue series might represent a degradation product formation in middle distillates.

Beaver and coauthors[14] demonstrated that a possible mass for SMORS-type degradation products is 317 Da, corresponding to a molecular formula of $C_{21}H_{19}O_2N$. Sobkowiak et al.[11] reported that these compounds result from the oxidation of quinone species and subsequent coupling reactions with nitrogen compounds. With these results, MS/MS measurements were performed to obtain structural information about the ions m/z 139.11192, 338.34149, and 675.67603, and the profile MS/MS of these ions is described in Figures S7−S9 (Supporting Information), respectively.

An interesting finding when observing these ions' fragmentation profile is the occurrence of the possible coupling reaction as reported by Sobkowiak et al.[11] The MS/MS profile of the ion m/z 675.67603 demonstrated the loss of −337 Da corresponding to $C_{22}H_{43}ON$ (Figure S9, see the Supporting Information) resulting in the ion m/z 338.34149 ($C_{22}H_{44}ON^+$). Additionally, the MS/MS profile of the ion m/z 338.34149, Figure S8 (see the Supporting Information), showed losses of −17 Da (NH_3) and −18 Da (H_2O), and subsequent dealkylation with losses of −14 Da corresponds to CH_2 units from its structure. In a similar manner, the ion m/z 139.11192 presented losses of −18 Da (H_2O) and −42 Da (C_3H_6). From the latter, a dealkylation was observed with losses of −14 Da (CH_2), as illustrated in Figure S7 (see the Supporting Information). The isotopic structure of these intense ions can be found in Figure S10 (see the Supporting Information).

These results suggest the presence of a single precursor species ($C_{22}H_{43}ON$) and highlight the possibility of a cyclic structure (C_5H_6O) with alkyl side chains with the probable organic functions: primary amine and secondary alcohol. The presence of the cyclic structure was suggested by the fragmentation of the m/z 129.11192 ion, resulting in the m/z 83.04917 fragment ion corresponding to $C_5H_7O^+$.

https://doi.org/10.1021/acsomega.3c08336
ACS Omega 2024, 9, 10415−10425

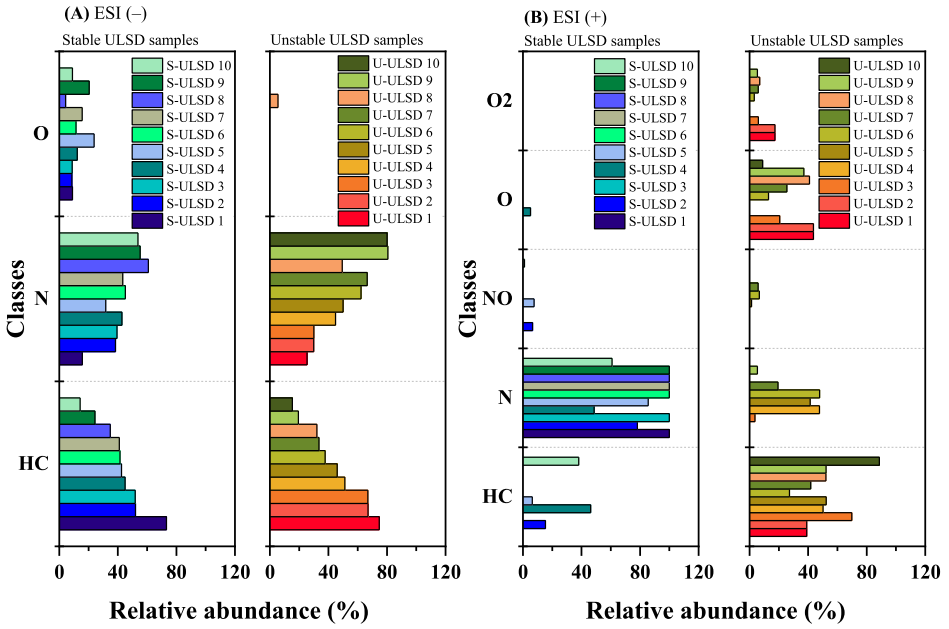

Figure 3. Class diagrams of the 20 ULSD samples (stable and unstable) analyzed by negative- (A) and positive-ion mode (B) ESI Orbitrap MS.

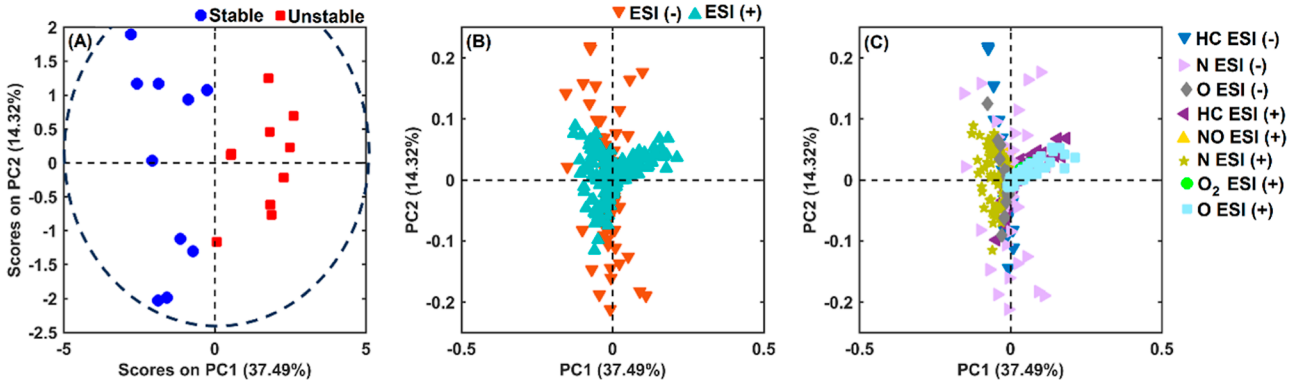

Figure 4. (A) Scores, (B) loadings (considering the ionization mode), and (C) loadings (identifying the classes of compounds) for the ESI (±) Orbitrap MS for 20 ULSD samples analyzed by PCA. The dashed ellipse delineates the 95% confidence region.

Generally, only the presence of aromatic nitrogen compounds is expected in petroleum-derived samples; however, a few studies have already reported the presence, even in low concentrations, of primary amines ($R-NH_2$) in these matrices.[59,60] In the case of ULSD, the presence of this functional group may be related to the HDT process from which this fuel is obtained.[60] Secondary alcohols are reported as possible auto-oxidation products of aromatic hydrocarbons.[61] The high molecular mass and low polarity presented by this compound point to the formation of a precursor species that can lead to the formation of gums and sediments in the fuel. The low DBE value presented by the ions discussed suggests that the degradation product differs from those observed in middle distillates leading to the formation of SMORS-type species with a high DBE value.

The analysis by ESI (±) Orbitrap MS allowed a detailed view at the molecular level of ULSD samples, and eight classes of compounds were identified, with three classes (HC, N, and O) accessed by ESI (−) and five classes (HC, N, NO, O, and O_2) accessed by ESI (+) HR-MS, as shown in Figure 3A. The PCA method was applied to individual compounds detected across both ionization modes to investigate which compound type is most significant for classifying ULSD samples in relation to the storage stability according to ASTM D5304.

Figure 4A shows the PC1 × PC2 scores for the 20 ULSD samples. Considering the two main components, 51.81% of the data variance was explained. The dashed ellipse delineates the 95% confidence region in the PCA score plot. The separation of stable and unstable ULSD samples is mainly observed by PC1 (37.49%). It can be seen from the analysis of the loadings illustrated in Figure 4B that considering only the information regarding the ionization mode is not possible to discriminate the variables that most influence the separation between the two sets of the ULSD samples.

Even though, by identifying the variables into classes of compounds (loadings in Figure 4C), a tendency was observed toward distinguishing the variables that best categorize the two sets of ULSD samples. To provide a clearer insight concerning the influence of each class of compounds on the discrimination between stable and unstable ULSD samples, the loadings were plotted individually for each variable class and are illustrated in Figure S11 (see the Supporting Information).

In ESI (−) analysis, the apparent difference between the set of ULSD samples was the class O detection in stable samples.

https://doi.org/10.1021/acsomega.3c08336
ACS Omega 2024, 9, 10415−10425

The DBE and carbon number distribution for this class can be seen in Figure 5. The detection of species with DBE values

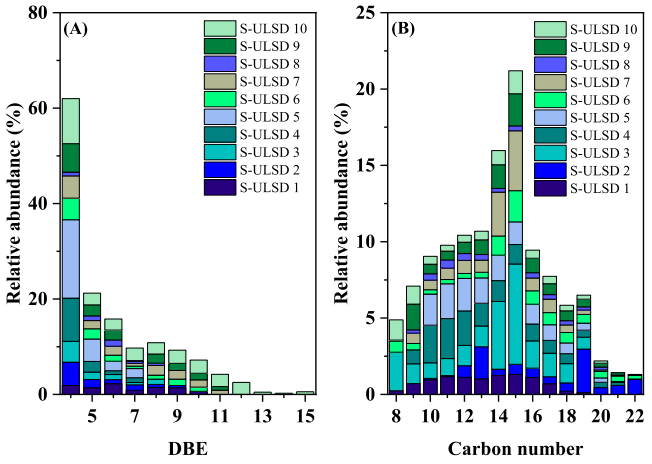

Figure 5. Distribution graphs of DBE (A) and carbon number (B) for the O class detected for stable ULSD samples analyzed by ESI (−) FT MS.

higher than 4 indicates the presence of alkylphenols, which have the hydroxyl functional group (−OH), which undergoes deprotonation when analyzed by ESI (−).[62]

The fuel oxygen consumption rate is inferior in fuels with a high concentration of natural antioxidants (i.e., phenols and thiols) since they are the primary reaction sites with peroxyl radicals. Thus, the peroxyl radical chain is inhibited, which characterizes stable fuels.[63] On the other hand, fuels with low levels of natural antioxidant compounds might present reactive characteristics for the formation of precipitates during a long storage period. For instance, these compounds will have limited ability to preserve the second most reactive compounds: hydrocarbons and other heterocompounds.[64]

Figure 3B illustrates the ESI (+) Orbitrap MS class diagram and highlights a predominance of basic nitrogen compound detection for the stable ULSD samples. These compounds do not influence the formation of gums and sediments in middle distillates.[20,42,65−68] Nevertheless, the absence of this class in most of the unstable ULSD samples may have contributed to the unstable performance when the ULSD samples were subjected to the induced storage test according to ASTM D5304. These results imply that such classes of compounds can be investigated in the search for new additives that increase the lifetime of the fuel.[69]

On the other hand, the loadings for the HC, O, and O_2 classes mainly categorize the unstable ULSD samples, as shown in Figure S11B (see the Supporting Information). In the class distribution graph illustrated in Figure 3B, hydrocarbons and oxygenated compounds were predominantly detected among the unstable ULSD samples. The oxygenated compounds may result from hydrocarbon oxidation generating hydroperoxides, which can react again with native compounds in middle distillates, producing oxygenated compounds such as alcohols and aldehydes.[70]

Hydrocarbons were detected by ESI in both ionization modes. The detection of this class of compounds is also related to the low content of polar constituents in ULSD samples, which contributes to reduce the ion suppression effect of polar compounds on hydrocarbons, enabling their ionization and subsequent detection of that class.[71] In ESI (−) analysis, the HC class refers to the presence of hydrocarbons with a Csp^3, which promotes deprotonation due to the formation of an aromatic carbanion that is stabilized by resonance.[72]

The ionization of hydrocarbons by ESI (+) is a more complex process and involves factors related to the composition of the matrix and, above all, the ionization process characteristic of ESI.[73,74] In a study reported by Schneider et al., the ionization of polyaromatic hydrocarbons led to the formation of ions of the $[M + H]^+$ type. The authors concluded that the low polar content characteristic of the matrix studied is the main factor corroborating the detection of hydrocarbons by ESI.[71] In the present study, the distribution of DBE for the HC class, illustrated in Figure S12 for the negative- and positive-ion mode, showed the detection of aromatic species with DBE greater than 4, corroborating the results reported by Schneider et al.

The DBE distributions for the HC class detected by ESI (±) showed the presence of naphthenoaromatic hydrocarbons among the ULSD samples. These compounds have aromatic and naphthenic rings in their chemical structures, mostly consisting of six- or five-membered rings.[55] According to Yang et al., these compounds are common in refined products from crude oil because polyaromatic hydrocarbons are also subjected to the hydrogenation process, which often takes place partially.[75] The hydrogenation mechanism involves a series of reversible reactions, where the hydrogenation of the first ring of fused aromatic hydrocarbons is relatively easy, while the hydrogenation of the last aromatic ring is more difficult.[76]

The detection of naphthenoaromatic hydrocarbons among the unstable ULSD samples suggests that this class of compounds is a relevant criterion in understanding the predisposition to instability observed for this group. The benzyl hydrogens present in the chemical structure of naphthenoaromatic hydrocarbons are susceptible to abstraction for the formation of organic radicals. This susceptibility is more probable because the formed radical will be stabilized by the resonance effect. Therefore, the organic radical will react according to the propagation steps in a radical-free mechanism and as a result, there is the formation of oxygenated species such as alcohols.[57,77]

A potential oxidation mechanism for a naphthenoaromatic hydrocarbon is illustrated in Scheme 1. The first step in this mechanism is the formation of an organic radical from the abstraction of hydrogen in the presence of light or heat. This radical tends to react with an O_2 molecule, giving rise to the peroxyl radical. In synthesis, the abstraction of a hydrogen radical from hydrocarbons or heterocompounds present in the fuel leads to the formation of hydroperoxide. This can decompose and produce other radicals. These radicals continue to react, composed of the propagation steps of the radical reaction, from which more complex oxygenated products are obtained. These products can also react in the presence of other compounds present in the fuel, leading to the formation of gums and deposits in the fuel.[57] The proposed mechanism also demonstrates the formation of O and O_2 species from a hydrocarbon molecule, suggesting that the latter is degradation products.

4. CONCLUSIONS

Preliminary experiments employing elemental analysis, GC × GC-FID, and ESI Orbitrap MS were conducted to study the chemical composition effect on ULSD stability. The elemental

https://doi.org/10.1021/acsomega.3c08336
ACS Omega 2024, 9, 10415−10425

Scheme 1. Proposed Radical Mechanism for the Oxidation of an Aromatic Naphthene Hydrocarbon with DBE 9[a]

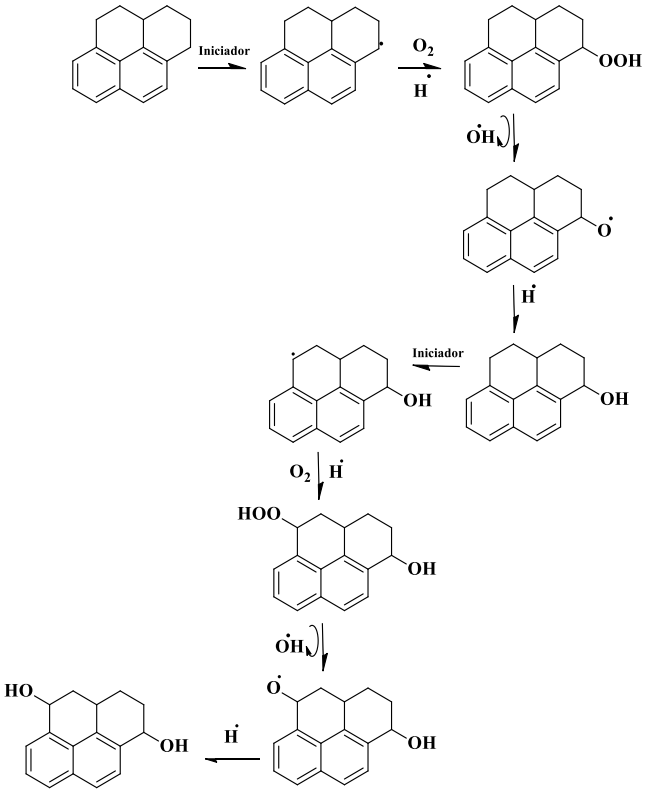

[a]The reaction is initiated by different factors such as the presence of light and/or heat.

analysis provided the contents of the main elements present in the ULSD samples. Nevertheless, by employing only this analysis, the differentiating of the samples regarding their stability could not be achieved.

On the other hand, using GC × GC-FID was possible to determine the main hydrocarbon classes in ULSD samples and their discrimination based on storage stability by applying the PCA model. Roughly 95% of the data variance was explained, indicating a clear separation between the two groups of samples analyzed. The GC × GC-FID data combined with PCA described that the separation of the samples' concerning stability was mainly due to the contents of mono- and diaromatic compounds present in the unstable ULSD samples.

However, the polar composition is not accessed by employing this method. Hence, polar compounds were evaluated using ESI in both ionization modes. Moreover, due to their low content in the ULSD fuel, the ionization of aromatic hydrocarbons was also possible. Thus, the nonpolar and polar compounds' impact on fuel stability could be assessed by ESI (±). PCA was also applied to the ESI data set, and the results highlight the presence of natural antioxidants, such as those belonging to the O class, which decrease the fuel oxygen consumption rate, characterizing it as stable composition.

Conversely, the oxidation and coupling reaction of naphthenoaromatic hydrocarbons with reactive polar compounds are the main routes to gum and deposit formation. Therefore, HDT is an important factor in the stability of ULSD samples. Furthermore, the MS/MS experiments indicate that the coupling reactions occurred for possible degradation product formation. The MS/MS experiments also highlight the presence of a single precursor species, which is the result of a coupling reaction between the HDT byproducts and the oxidation of unsaturated hydrocarbons. In summary, this is one of the first studies to integrate different analytical techniques combined with chemometric approaches to analyze the chemical composition of a low-polar content fuel in order to investigate its stability over storage time.

■ ASSOCIATED CONTENT

Supporting Information

The Supporting Information is available free of charge at https://pubs.acs.org/doi/10.1021/acsomega.3c08336.

Scheme of SMORS formation; elemental composition of the ULSD samples; content of the main hydrocarbon classes accessed by GC × GC-FID; number of peaks assigned and % assigned for all ULSD samples analyzed by ESI (±) Orbitrap MS; distribution plots of the carbon number vs the content of the main hydrocarbon classes for the stable and unstable ULSD samples accessed by GC × GC-FID; error distribution as a function of m/z for the stable and unstable ULSD samples analyzed by ESI (±) Orbitrap MS; high-resolution MS/MS experiments (CID) of the isolated ions m/z 139.11192, 338.34149, and 675.67617; isotopic structure (sample and theoretical) of the ions (A) m/z 139.11199, (B) m/z 338.34166, and (C) m/z 675.67603; contour plots of DBE vs the carbon number for all classes detected by ESI (±) Orbitrap MS for the representative (A) stable and (B) unstable ULSD samples; ESI (±) mass spectrum of the variables used as input in the PCA model; and loadings with the classes of compounds identified for the ESI (±) Orbitrap MS for 20 ULSD samples analyzed by PCA (PDF)

■ AUTHOR INFORMATION

Corresponding Authors

Jussara V. Roque − *Laboratory of Chromatography and Mass Spectrometry, Institute of Chemistry, Federal University of Goiás, Goiânia, Goiânia 74001-970, Brazil;* orcid.org/0000-0002-5220-959X; Email: jussararoque@gmail.com

Boniek G. Vaz − *Laboratory of Chromatography and Mass Spectrometry, Institute of Chemistry, Federal University of Goiás, Goiânia, Goiânia 74001-970, Brazil;* orcid.org/0000-0003-1197-4284; Email: boniek@ufg.br

Authors

Deborah V. A. de Aguiar − *Laboratory of Chromatography and Mass Spectrometry, Institute of Chemistry, Federal University of Goiás, Goiânia, Goiânia 74001-970, Brazil;* orcid.org/0000-0002-8769-1339

Leomir A. S. de Lima − *Laboratory of Chromatography and Mass Spectrometry, Institute of Chemistry, Federal University of Goiás, Goiânia, Goiânia 74001-970, Brazil*

Iris M. Junior − *CENPES, PETROBRAS, Rio de Janeiro, Rio de Janeiro 21941-915, Brazil*

Helineia O. Gomes − *CENPES, PETROBRAS, Rio de Janeiro, Rio de Janeiro 21941-915, Brazil*

Emanoel N. R. de Sousa − *CENPES, PETROBRAS, Rio de Janeiro, Rio de Janeiro 21941-915, Brazil*

Gláucia P. L. Piccoli − *CENPES, PETROBRAS, Rio de Janeiro, Rio de Janeiro 21941-915, Brazil*

https://doi.org/10.1021/acsomega.3c08336
ACS Omega 2024, 9, 10415−10425

Complete contact information is available at:
https://pubs.acs.org/10.1021/acsomega.3c08336

Author Contributions

All authors have given approval to the final version of the manuscript.

Funding

The authors acknowledge financial support from Petróleo Brasileiro SA-Petrobras, Coordenação de Aperfeiçoamento de Pessoal de Nível Superior (CAPES), and Conselho Nacional de Desenvolvimento Científico e Tecnológico (CNPq).

Notes

The authors declare no competing financial interest.

NOMENCLATURE

AGC, automatic gain control; DBE, double-bond equivalent; ESI, electrospray ionization; GC × GC FID, comprehensive two-dimensional gas chromatography with a flame ionization detector; HCD, energy collision dissociation; HESI, heated electrospray ionization source; HDT, hydrotreatment; HR-MS, high-resolution mass spectrometry; IT, injection time; NCE, normalized collision energy; PC, principal component; PCA, principal component analysis; SMORS, soluble macromolecular oxidatively reactive species; ULSD, ultralow-sulfur diesel

REFERENCES

(1) Cooper, J. Fuels Europe. Refining Products for Our Everyday Life *Statistical Report*, 2018.
(2) US Department of Energy. *Petroleum & Other Liquids*.
(3) Chakravarthy, R.; Acharya, C.; Savalia, A.; Naik, G. N.; Das, A. K.; Saravanan, C.; Verma, A.; Gudasi, K. B. Property Prediction of Diesel Fuel Based on the Composition Analysis Data by Two-Dimensional Gas Chromatography. *Energy Fuels* **2018**, *32* (3), 3760−3774.
(4) Richter, F. P.; Caesar, P. D.; Meisel, S. L.; Offenhauer, R. D. Distribution of Nitrogen in Petroleum According to Basicity. *Ind. Eng. Chem.* **1952**, *44* (11), 2601−2605.
(5) Mushrush, G. W.; Beal, E. J.; Hazlett, R. N.; Hardy, D. R. Chemical Basis of Instability of Shale-Derived Middle Distillate Fuels: A Model Study of the Interactive Effects between 2,5-Dimethylpyrrole and 3-Methylindole with Sulfonic and Carboxylic Acids. *Energy Fuels* **1991**, *5* (5), 749−753.
(6) Hazlett, R. N.; Power, A. J. Phenolic Compounds in Bass Strait Distillate Fuels: Their Effect on Deposit Formation. *Fuel* **1989**, *68* (9), 1112−1117.
(7) Hardy, D. R.; Wechter, M. A. Insoluble Sediment Formation in Middle-Distillate Diesel Fuel: The Role of Soluble Macromolecular Oxidatively Reactive Species. *Energy Fuels* **1990**, *4* (3), 270−274.
(8) Gül, Ö.; Cetiner, R.; Griffith, J. M.; Wang, B.; Sobkowiak, M.; Fonseca, D. A.; Aksoy, P.; Miller, B. G.; Beaver, B. Insight into the Mechanisms of Middle Distillate Fuel Oxidative Degradation. Part 3: Hydrocarbon Stabilizers to Improve Jet Fuel Thermal Oxidative Stability. *Energy Fuels* **2009**, *23* (4), 2052−2055.
(9) ASTM International. Thermal Oxidation Stability of Aviation Fuels. *ASTM D943-99*: West Conshohocken, 1991.
(10) Kabana, C. G.; Botha, S.; Schmucker, C.; Woolard, C.; Beaver, B. Oxidative Stability of Middle Distillate Fuels. Part 1: Exploring the Soluble Macromolecular Oxidatively Reactive Species (SMORS) Mechanism with Jet Fuels. *Energy Fuels* **2011**, *25* (11), 5145−5157.
(11) Sobkowiak, M.; Griffith, J. M.; Wang, B.; Beaver, B. Insight into the Mechanisms of Middle Distillate Fuel Oxidative Degradation. Part 1: On the Role of Phenol, Indole, and Carbazole Derivatives in the Thermal Oxidative Stability of Fischer−Tropsch/Petroleum Jet Fuel Blends. *Energy Fuels* **2009**, *23* (4), 2041−2046.
(12) Johnson, D. W. The Effects of Storage on Turbine Engine Fuels. In *Flight Physics—Models, Techniques and Technologies*; InTech, 2018..
(13) Aksoy, P.; Gül, Ö.; Cetiner, R.; Fonseca, D. A.; Sobkowiak, M.; Falcone-Miller, S.; Miller, B. G.; Beaver, B. Insight into the Mechanisms of Middle Distillate Fuel Oxidative Degradation. Part 2: On the Relationship between Jet Fuel Thermal Oxidative Deposit, Soluble Macromolecular Oxidatively Reactive Species, and Smoke Point. *Energy Fuels* **2009**, *23* (4), 2047−2051.
(14) Beaver, B.; Gao, L.; Burgess-Clifford, C.; Sobkowiak, M. On the Mechanisms of Formation of Thermal Oxidative Deposits in Jet Fuels. Are Unified Mechanisms Possible for Both Storage and Thermal Oxidative Deposit Formation for Middle Distillate Fuels? *Energy Fuels* **2005**, *19* (4), 1574−1579.
(15) Balster, L. M.; Zabarnick, S.; Striebich, R. C.; Shafer, L. M.; West, Z. J. Analysis of Polar Species in Jet Fuel and Determination of Their Role in Autoxidative Deposit Formation. *Energy Fuels* **2006**, *20* (6), 2564−2571.
(16) Siddiquee, M. N.; de Klerk, A. Heterocyclic Addition Reactions during Low Temperature Autoxidation. *Energy Fuels* **2015**, *29* (7), 4236−4244.
(17) ASTM International. Standard Test Method for Oxidation Stability of Distillate Fuel Oil. *ASTM D2274-14*: West Conshohocken, 2019.
(18) ASTM International. Standard Test Method for Assessing Middle Distillate Fuel Storage Stability by Oxygen Overpressure. *ASTM D5304-15*: West Conshohocken, 2015.
(19) Batts, B. D.; Fathoni, A. Z. A Literature Review on Fuel Stability Studies with Particular Emphasis on Diesel Oil. *Energy Fuels* **1991**, *5* (1), 2−21.
(20) Romanczyk, M.; Loegel, T. N.; Myers, K. M. Qualitative Characterization of Nitrogen-Containing Compounds in Jet and Diesel Fuel Extracts by Using (+) Electrospray Ionization Coupled to a Linear Quadrupole Ion Trap/Orbitrap Mass Spectrometer. *Fuel* **2023**, *344*, 128062.
(21) Safa, M. A.; Ma, X.; Bouresli, R.; Albazzaz, H. Effects of Co-Existing Nitrogen Compounds and Polycyclic Aromatic Hydrocarbons on Catalytic Oxidative Desulfurization of Refractory Sulfur Compounds in Middle Distillates. *Catal. Today* **2021**, *371*, 258−264.
(22) Deese, R. D.; Morris, R. E.; Metz, A. E.; Myers, K. M.; Johnson, K.; Loegel, T. N. Characterization of Organic Nitrogen Compounds and Their Impact on the Stability of Marginally Stable Diesel Fuels. *Energy Fuels* **2019**, *33* (7), 6659−6669.
(23) Stanislaus, A.; Marafi, A.; Rana, M. S. Recent Advances in the Science and Technology of Ultra Low Sulfur Diesel (ULSD) Production. *Catal. Today* **2010**, *153* (1−2), 1−68.
(24) Novák, M.; Palya, D.; Bodai, Z.; Nyiri, Z.; Magyar, N.; Kovács, J.; Eke, Z. Combined Cluster and Discriminant Analysis: An Efficient Chemometric Approach in Diesel Fuel Characterization. *Forensic Sci. Int.* **2017**, *270*, 61−69.
(25) Odebunmi, E. O.; Ogunsakin, E. A.; Ilukhor, P. E. P. Characterisation of Crude Oils and Petroleum Products, (I) Elution Liquid Chromatographic Separation and Gas Chromatographic Analysis of Crude Oils and Petroleum Products. *Bull. Chem. Soc. Ethiop.* **2002**, *16* (2), 115−132.
(26) Jennerwein, M. K.; Sutherland, A. C.; Eschner, M.; Gröger, T.; Wilharm, T.; Zimmermann, R. Quantitative Analysis of Modern Fuels Derived from Middle Distillates—The Impact of Diverse Compositions on Standard Methods Evaluated by an Offline Hyphenation of HPLC-Refractive Index Detection with GC × GC-TOFMS. *Fuel* **2017**, *187*, 16−25.
(27) Šindelářová, L.; Luu, E. N.; Vozka, P. Comparison of Gas and Kerosene Oils Chemical Composition before and after Hydrotreating Using Comprehensive Two-Dimensional Gas Chromatography. *J. Chromatogr. Open* **2022**, *2*, 100068.
(28) Ávila, B. M.; Pereira, V. B.; Gomes, A. O.; Azevedo, D. A. Speciation of Organic Sulfur Compounds Using Comprehensive Two-Dimensional Gas Chromatography Coupled to Time-of-Flight

Mass Spectrometry: A Powerful Tool for Petroleum Refining. *Fuel* **2014**, *126*, 188−193.
(29) Genuit, W.; Chaabani, H. Comprehensive Two-Dimensional Gas Chromatography-Field Ionization Time-of-Flight Mass Spectrometry (GC × GC-FI-TOFMS) for Detailed Hydrocarbon Middle Distillate Analysis. *Int. J. Mass Spectrom.* **2017**, *413*, 27−32.
(30) Jennerwein, M. K.; Eschner, M.; Gröger, T.; Wilharm, T.; Zimmermann, R. Complete Group-Type Quantification of Petroleum Middle Distillates Based on Comprehensive Two-Dimensional Gas Chromatography Time-of-Flight Mass Spectrometry (GC × GC-TOFMS) and Visual Basic Scripting. *Energy Fuels* **2014**, *28* (9), 5670−5681.
(31) Jennerwein, M.; Eschner, M.; Wilharm, T.; Gröger, T.; Zimmermann, R. Evaluation of Reversed Phase versus Normal Phase Column Combination for the Quantitative Analysis of Common Commercial Available Middle Distillates Using GC × GC-TOFMS and Visual Basic Script. *Fuel* **2019**, *235*, 336−338.
(32) Vozka, P.; Mo, H.; Šimáček, P.; Kilaz, G. Middle Distillates Hydrogen Content via GC × GC-FID. *Talanta* **2018**, *186*, 140−146.
(33) Hughey, C. A.; Rodgers, R. P.; Marshall, A. G. Resolution of 11000 Compositionally Distinct Components in a Single Electrospray Ionization Fourier Transform Ion Cyclotron Resonance Mass Spectrum of Crude Oil. *Anal. Chem.* **2002**, *74* (16), 4145−4149.
(34) Schmidt, E. M.; Pudenzi, M. A.; Santos, J. M.; Angolini, C. F. F.; Pereira, R. C. L.; Rocha, Y. S.; Denisov, E.; Damoc, E.; Makarov, A.; Eberlin, M. N. Petroleomics via Orbitrap Mass Spectrometry with Resolving Power above 1000000 at m/z 200. *RSC Adv.* **2018**, *8* (11), 6183−6191.
(35) Cho, Y.; Ahmed, A.; Islam, A.; Kim, S. Developments in FT-ICR MS Instrumentation, Ionization Techniques, and Data Interpretation Methods for Petroleomics. *Mass Spectrom. Rev.* **2015**, *34*, 248−263.
(36) Pomerantz, A. E.; Mullins, O. C.; Paul, G.; Ruzicka, J.; Sanders, M. Orbitrap Mass Spectrometry: A Proposal for Routine Analysis of Nonvolatile Components of Petroleum. *Energy Fuels* **2011**, *25* (7), 3077−3082.
(37) Marshall, A. G.; Rodgers, R. P. Petroleomics: The Next Grand Challenge for Chemical Analysis. *Acc. Chem. Res.* **2004**, *37* (1), 53−59.
(38) Stanford, L. A.; Kim, S.; Rodgers, R. P.; Marshall, A. G. Characterization of Compositional Changes in Vacuum Gas Oil Distillation Cuts by Electrospray Ionization Fourier Transform-Ion Cyclotron Resonance (FT-ICR) Mass Spectrometry. *Energy Fuels* **2006**, *20* (4), 1664−1673.
(39) Vanini, G.; Barra, T. A.; Souza, L. M.; Madeira, N. C. L.; Gomes, A. O.; Romão, W.; Azevedo, D. A. Characterization of Nonvolatile Polar Compounds from Brazilian Oils by Electrospray Ionization with FT-ICR MS and Orbitrap-MS. *Fuel* **2020**, *282*, 118790.
(40) de Aguiar, D. V. A.; da Silva Lima, G.; da Silva, R. R.; Júnior, I. M.; Gomes, A. d. O.; Mendes, L. A. N.; Vaz, B. G. Comprehensive Composition and Comparison of Acidic Nitrogen- and Oxygen-Containing Compounds from Pre- and Post-Salt Brazilian Crude Oil Samples by ESI (−) FT-ICR MS. *Fuel* **2022**, *326*, 125129.
(41) Commodo, M.; Fabris, I.; Groth, C. P. T.; Gülder, Ö. L. Analysis of Aviation Fuel Thermal Oxidative Stability by Electrospray Ionization Mass Spectrometry (ESI-MS). *Energy Fuels* **2011**, *25* (5), 2142−2150.
(42) Epping, R.; Kerkering, S.; Andersson, J. T. Influence of Different Compound Classes on the Formation of Sediments in Fossil Fuels During Aging. *Energy Fuels* **2014**, *28* (9), 5649−5656.
(43) Inan, T. Y.; Al-Hajji, A.; Koseoglu, O. R. Chemometrics-Based Analytical Method Using FTIR Spectroscopic Data To Predict Diesel and Diesel/Diesel Blend Properties. *Energy Fuels* **2016**, *30* (7), 5525−5536.
(44) Johnson, K. J.; Rose-Pehrsson, S. L.; Morris, R. E. Monitoring Diesel Fuel Degradation by Gas Chromatography-Mass Spectroscopy and Chemometric Analysis. *Energy Fuels* **2004**, *18* (3), 844−850.
(45) Hupp, A. M.; Marshall, L. J.; Campbell, D. I.; Smith, R. W.; McGuffin, V. L. Chemometric Analysis of Diesel Fuel for Forensic and Environmental Applications. *Anal. Chim. Acta* **2008**, *606* (2), 159−171.
(46) Karonis, D.; Zahos-Siagos, I.; Filimon, D.; Vasileiou, F. A Multivariate Statistical Analysis to Evaluate and Predict Ignition Quality of Marine Diesel Fuel Distillates from Their Physical Properties. *Fuel Process. Technol.* **2017**, *166*, 299−311.
(47) Moura, H. O. M. A.; Câmara, A. B. F.; Santos, M. C. D.; Morais, C. L. M.; de Lima, L. A. S.; Lima, K. M. G.; de Carvalho, L. S. Advances in Chemometric Control of Commercial Diesel Adulteration by Kerosene Using IR Spectroscopy. *Anal. Bioanal. Chem.* **2019**, *411* (11), 2301−2315.
(48) Bro, R.; Smilde, A. K. Principal Component Analysis. *Anal. Methods* **2014**, *6* (9), 2812−2831.
(49) Corgozinho, C.; Pasa, V.; Barbeira, P. Determination of Residual Oil in Diesel Oil by Spectrofluorimetric and Chemometric Analysis. *Talanta* **2008**, *76* (2), 479−484.
(50) *ASTM D5304. Standard Test Method for Assessing Middle Distillate Fuel Storage Stability by Oxygen Overpressure*; ASTM (American Society for Testing and Materials International), 2016; Vol. *14*; pp 1−5.
(51) *ASTM D5762-18. Standard Test Method for Nitrogen in Liquid Hydrocarbons, Petroleum and Petroleum Products by Boat-Inlet Chemiluminescence*; ASTM International, 2018; p 6..
(52) *ASTM D5291-1. Carbon, Hydrogen, and Nitrogen in Petroleum Products and Lubricants*; ASTM International, 2015; p 6..
(53) Filewood, T.; Kwok, H.; Brunswick, P.; Yan, J.; Ollinik, J. E.; Cote, C.; Kim, M.; van Aggelen, G.; Helbing, C. C.; Shang, D. A Rapid Gas Chromatography Quadrupole Time-of-Flight Mass Spectrometry Method for the Determination of Polycyclic Aromatic Hydrocarbons and Sulfur Heterocycles in Spilled Crude Oils. *Anal. Methods* **2022**, *14* (7), 717−725.
(54) Vendeuvre, C.; Ruiz-Guerrero, R.; Bertoncini, F.; Duval, L.; Thiébaut, D.; Hennion, M.-C. Characterisation of Middle-Distillates by Comprehensive Two-Dimensional Gas Chromatography (GC × GC): A Powerful Alternative for Performing Various Standard Analysis of Middle-Distillates. *J. Chromatogr. A* **2005**, *1086* (1−2), 21−28.
(55) Yang, C.; Faragher, R.; Yang, Z.; Hollebone, B.; Fieldhouse, B.; Lambert, P.; Beaulac, V. Characterization of Chemical Fingerprints of Ultralow Sulfur Fuel Oils Using Gas Chromatography-Quadrupole Time-of-Flight Mass Spectrometry. *Fuel* **2023**, *343*, 127948.
(56) DeWitt, M. J.; West, Z.; Zabarnick, S.; Shafer, L.; Striebich, R.; Higgins, A.; Edwards, T. Effect of Aromatics on the Thermal-Oxidative Stability of Synthetic Paraffinic Kerosene. *Energy Fuels* **2014**, *28* (6), 3696−3703.
(57) Jia, T.; Pan, L.; Wang, X.; Xie, J.; Gong, S.; Fang, Y.; Liu, H.; Zhang, X.; Zou, J.-J. Mechanistic Insights into the Thermal Oxidative Deposition of C10 Hydrocarbon Fuels. *Fuel* **2021**, *285*, 119136.
(58) Sharma, Y. K. The Instability of Storage of Middle Distillate Fuels: A Review. *Pet. Sci. Technol.* **2012**, *30* (17), 1839−1850.
(59) Cho, Y.; Ahmed, A.; Kim, S. Application of Atmospheric Pressure Photo Ionization Hydrogen/Deuterium Exchange High-Resolution Mass Spectrometry for the Molecular Level Speciation of Nitrogen Compounds in Heavy Crude Oils. *Anal. Chem.* **2013**, *85* (20), 9758−9763.
(60) Prado, G. H. C.; Rao, Y.; De Klerk, A. Nitrogen Removal from Oil: A Review. *Energy Fuels* **2017**, *31* (1), 14−36.
(61) Zabarnick, S.; Phelps, D. K. Density Functional Theory Calculations of the Energetics and Kinetics of Jet Fuel Autoxidation Reactions. *Energy Fuels* **2006**, *20* (2), 488−497.
(62) Rocha, Y. d. S.; Pereira, R. C. L.; Mendonça Filho, J. G. Geochemical Assessment of Oils from the Mero Field, Santos Basin, Brazil. *Org. Geochem.* **2019**, *130*, 1−13.
(63) Heneghan, S. P.; Zabarnick, S. Oxidation of Jet Fuels and the Formation of Deposit. *Fuel* **1994**, *73* (1), 35−43.

https://doi.org/10.1021/acsomega.3c08336
ACS Omega 2024, 9, 10415−10425

(64) Kendall, D. R.; Mills, J. S. Thermal Stability of Aviation Kerosines: Techniques to Characterize their Oxidation Properties. *Ind. Eng. Chem. Prod. Res. Dev.* **1986**, *25* (2), 360−366.
(65) Bauserman, J. W.; Mushrush, G. W.; Hardy, D. R. Organic Nitrogen Compounds and Fuel Instability in Middle Distillate Fuels. *Ind. Eng. Chem. Res.* **2008**, *47* (9), 2867−2875.
(66) Thompson, R. B.; Druge, L. W.; Chenicek, J. A. Stability of Fuel Oils in Storage: Effect of Sulfur Compounds. *Ind. Eng. Chem.* **1949**, *41* (12), 2715−2721.
(67) Adams, C.; Alborzi, E.; Meijer, A. J. H. M.; Hughes, K. J.; Pourkashanian, M. Mechanistic Investigation into the Formation of Insolubles in Bulk Fuel Jet Fuel Using Quantum Chemical and Experimental Techniques. *Fuel* **2023**, *334*, 126202.
(68) Ashraful, A. M.; Masjuki, H. H.; Kalam, M. A.; Rahman, S. M. A.; Habibullah, M.; Syazwan, M. Study of the Effect of Storage Time on the Oxidation and Thermal Stability of Various Biodiesels and their Blends. *Energy Fuels* **2014**, *28* (2), 1081−1089.
(69) Mikhaylova, P.; de Oliveira, L. P.; Merdrignac, I.; Berlioz-Barbier, A.; Nemri, M.; Giusti, P.; Pirngruber, G. D. Molecular Analysis of Nitrogen-Containing Compounds in Vacuum Gas Oils Hydrodenitrogenation by (ESI+/−)-FTICR-MS. *Fuel* **2022**, *323*, 124302.
(70) Boryaev, A. A. Development of Advanced Methods of Determining the Chemical Stability of Hydrocarbon Fuels. *Thermochim. Acta* **2020**, *685*, 178508.
(71) Schneider, E.; Giocastro, B.; Rüger, C. P.; Adam, T. W.; Zimmermann, R. Detection of Polycyclic Aromatic Hydrocarbons in High Organic Carbon Ultrafine Particle Extracts by Electrospray Ionization Ultrahigh-Resolution Mass Spectrometry. *J. Am. Soc. Mass Spectrom.* **2022**, *33* (11), 2019−2023.
(72) Lobodin, V. V.; Juyal, P.; McKenna, A. M.; Rodgers, R. P.; Marshall, A. G. Tetramethylammonium Hydroxide as a Reagent for Complex Mixture Analysis by Negative Ion Electrospray Ionization Mass Spectrometry. *Anal. Chem.* **2013**, *85* (16), 7803−7808.
(73) Miyabayashi, K.; Naito, Y.; Tsujimoto, K.; Miyake, M. Structure Characterization of Polyaromatic Hydrocarbons in Arabian Mix Vacuum Residue by Electrospray Ionization Fourier Transform Ion Cyclotron Resonance Mass Spectrometry. *Int. J. Mass Spectrom.* **2004**, *235* (1), 49−57.
(74) Van Berkel, G. J.; McLuckey, S. A.; Glish, G. L. Electrochemical Origin of Radical Cations Observed in Electrospray Ionization Mass Spectra. *Anal. Chem.* **1992**, *64* (14), 1586−1593.
(75) Yang, C.; Wang, Z.; Yang, Z.; Hollebone, B.; Fieldhouse, B.; Lambert, P.; Fingas, M. 2 Chemical Fingerprints and Chromatographic Analysis of Crude Oils and Petroleum Products. In *The Chemistry of Oil and Petroleum Products*; De Gruyter, 2022; pp 47−126..
(76) Banerjee, S.; Mani, K.; Leonard, L.; Kokayeff, P. Distillate Hydrotreating to Ultra-Low-Sulfur Diesel—The Impact of Aromatics. *Indian Chem. Eng.* **2011**, *53* (3), 152−169.
(77) Webster, R. L.; Rawson, P. M.; Kulsing, C.; Evans, D. J.; Marriott, P. J. Investigation of the Thermal Oxidation of Conventional and Alternate Aviation Fuels with Comprehensive Two-Dimensional Gas Chromatography Accurate Mass Quadrupole Time-of-Flight Mass Spectrometry. *Energy Fuels* **2017**, *31* (5), 4886−4894.

https://doi.org/10.1021/acsomega.3c08336
ACS Omega 2024, 9, 10415−10425